Charge Order, Dynamics, and Magnetostructural Transition in Multiferroic $LuFe_2O_4$

X. S. Xu,[1] M. Angst,[2,3] T. V. Brinzari,[1] R. P. Hermann,[3,4] J. L. Musfeldt,[1] A. D. Christianson,[2] D. Mandrus,[2,5] B. C. Sales,[2] S. McGill,[6] J.-W. Kim,[7] and Z. Islam[8]

[1]*Department of Chemistry, University of Tennessee, Knoxville, Tennessee 37996, USA*
[2]*Oak Ridge National Laboratory, Oak Ridge, Tennessee 37831, USA*
[3]*Institut für Festkörperforschung, Forschungszentrum Jülich GmbH, D-52425 Jülich, Germany*
[4]*Department of Physics, B5, Université de Liège, B-4000 Sart-Tilman, Belgium*
[5]*Department of Physics, University of Tennessee, Knoxville, Tennessee 37996, USA*
[6]*National High Magnetic Field Laboratory, Tallahassee, Florida, 32310, USA*
[7]*Ames Laboratory, Ames, Iowa 50010, USA*
[8]*Advanced Photon Source, Argonne National Laboratory, Argonne, Illinois 60439, USA*

(Received 16 September 2008; published 26 November 2008)

We investigated the series of temperature and field-driven transitions in $LuFe_2O_4$ by optical and Mössbauer spectroscopies, magnetization, and x-ray scattering in order to understand the interplay between charge, structure, and magnetism in this multiferroic material. We demonstrate that charge fluctuation has an onset well below the charge ordering transition, supporting the ''order by fluctuation'' mechanism for the development of charge order superstructure. Bragg splitting and large magneto-optical contrast suggest a low-temperature monoclinic distortion that can be driven by both temperature and magnetic field.

DOI: 10.1103/PhysRevLett.101.227602 PACS numbers: 76.80.+y, 71.30.+h, 75.30.Kz, 78.20.Ci

Complex oxides take advantage of the unique and flexible properties of transition metal centers to govern bonding and local structure. Further, the delicate interplay between charge, structure, and magnetism yields important consequences for functionality and cross coupling. Iron-based materials such as multiferroic $BiFeO_3$ and $LuFe_2O_4$ [1,2], bistable photomagnetic systems such as Prussian blues and related derivatives [3], dilute magnetic semiconductors [4], and the new family $LaFeAsO_{1-x}F_x$ of superconductors [5] have attracted recent attention, in this regard. In this Letter, we focus on $LuFe_2O_4$, a frustrated system with a series of phase transitions that give rise to electronically driven multiferroicity [6].

$LuFe_2O_4$ has a layered structure with Fe-containing double layers of triangular connectivity. Three-dimensional Fe^{2+}/Fe^{3+} charge order (CO) occurs below 320 K (T_{CO}). This is followed by ferrimagnetic order below 240 K (T_N) [2,7,8]. An additional low-temperature magnetic phase transition has recently been reported at 175 K (T_{LT}) [9]. The CO has a so-called $\sqrt{3} \times \sqrt{3}$ superstructure [7,8]. Because of the mixed valent iron centers and frustrated triangular lattice, the Fe^{2+} and Fe^{3+} populations are different within the double layer, an effect that renders the double layer intrinsically polar [2,8]. The charge ordering mechanism is thus central to understanding the unusual physical properties of this multiferroic.

To elucidate the charge excitations and understand how they correlate with structure and magnetism, we measured the optical and Mössbauer spectra, magnetization, and x-ray scattering of $LuFe_2O_4$. We compare our comprehensive results to recent electronic structure calculations [7] and to spectral data on classical magnetite [10]. We demonstrate that strong $Fe^{2+} \rightarrow Fe^{3+}$ charge fluctuation persists even in charge ordered states characterized by superstructure reflections, and it persists down to T_{LT} below which Bragg splitting indicates that strong monoclinic distortions occur. These observations are consistent with the ''order by fluctuation'' mechanism [11], in which case $\sqrt{3} \times \sqrt{3}$ CO is preferable for entropy reasons and stabilized by the charge fluctuation in this geometrically frustrated system. As in magnetite, we analyze the results in terms of a polaron picture, extracting a large effective mass for the charge carriers. On the other hand, Fe^{2+} on-site excitations are sensitive to the magnetic transition at T_{LT} and display a sizable magneto-optical effect. Combining our spectral, magnetic, and structural data, we generate an H-T phase diagram and show that the transition at T_{LT} can also be driven by a magnetic field. These results demonstrate the important interplay between charge, structure, and magnetism.

All experiments were conducted on floating-zone-grown $LuFe_2O_4$ single crystals from the same batch as those used in Refs. [8,9]. Near-normal reflectance measurements were carried out on ab plane samples employing a series of spectrometers covering a wide range of energy (30 meV–6.5 eV), temperature (4–540 K) and magnetic field (0–33 T, $H \parallel c$) [12]. Optical conductivity $\sigma_1(E)$ was calculated by a Kramers-Kronig analysis [13]. Variable temperature transmittance was done on a 25 μm ab plane crystal, allowing direct calculation of absorption $\alpha(E)$. The ^{57}Fe Mössbauer spectra of 35 mg/cm^2 of crushed crystals were recorded between 260 and 400 K on a constant acceleration spectrometer with a Rh matrix Co-57 source and calibrated at 295 K with α-Fe powder. The reported isomer shifts are

relative to α-Fe at 295 K. X-ray scattering was performed at undulator beam line 4-ID-D at the Advanced Photon Source with 36 keV photons employing a cryostat with a split coil vertical field magnet up to 4 T. The sample was mounted with an angle of 45° between c and the field as a compromise between cryomagnet angular restrictions and accessibility of important regions of reciprocal space. Previous magnetization work shows that $LuFe_2O_4$ is rather insensitive to fields $\| ab$ below 7 T. Consequently, the dominate effect of the field is due to the component $\| c$.

The Mössbauer spectra, [Fig. 1(a)] were fit with a Blume-Tjon model [14] for Fe^{2+} and Fe^{3+} relaxation, similar to [15]. Individual fits of the spectra reveal (i) two Arrhenius processes as indicated by the temperature dependence of the hopping frequency and break at T_{CO} [Fig. 1(b)], (ii) the difference between Fe^{2+} and Fe^{3+} isomer shifts, $\Delta\delta$, is constant below T_{CO} and cannot be resolved above, and (iii) a constant linewidth and a gradual $\sim\sqrt{T_{CO}-T}$ broadening above and below T_{CO}, respectively. In order to overcome correlation effects (see below) and to reduce the large number of fit parameters, a simultaneous parametric fit of all spectra was then carried out with the constraints (i), (ii) constant $\Delta\delta$ for all T, and (iii). The fits in Fig. 1(a) are the result of this simultaneous fit. The obtained spectral parameters and relaxation frequencies [Figs. 1(b) and 1(c)] are in agreement with [15], with the exception of the sharper T dependence of these parameters around T_{CO}, which we attribute to the preparation of the sample as single crystal. Above T_{CO}, we obtained an activation energy of 0.16(2) eV. This is somewhat smaller than the 0.26 eV energy obtained by electrical conductivity measurements [15]. Below T_{CO}, we find the activation energy to be 0.36(9) eV. The large error bar is due to (i) small hopping frequencies, close to the detection limit, and (ii) correlations between the hopping frequency and linewidth. The Fe^{2+} line around 1.4 mm/s is increasingly broadened below T_{CO} due to microscopic lattice distortions in the charge ordered state [Fig. 1(a)] [15]. The fit at the bottom of Fig. 1(a) is the best fit with a constraint of 33% of $Fe^{2.5+}$ with a hopping frequency of 1 GHz. The poor fit quality indicates that the 260 K hopping frequency is smaller than 1 GHz, which invalidates the presence of 33% of $Fe^{2.5+}$ below T_{CO} suggested in Ref. [16] from modeling electron diffraction, a technique with a resolution better than 1 GHz.

To further study the charge fluctuation ($Fe^{2+} \rightarrow Fe^{3+}$ charge transfer) observed in Mössbauer spectroscopy, we employed optical spectroscopy, a technique in which hopping is driven by comparatively high frequency photons ($\sim 10^{14}$ Hz, in contrast to the natural hopping rate of a few MHz, as observed by Mössbauer spectroscopy). Figure 2(a) displays the optical conductivity of $LuFe_2O_4$. We assign the observed excitations based upon recent first principle calculations [7]. The lowest allowed electronic features are minority channel $Fe^{2+} \rightarrow Fe^{3+}$ charge transfer excitations. At slightly higher energy follow Fe^{2+} on-site excitations. Minority channel O $p \rightarrow$ Fe d charge transfer and overlapping majority channel O $p \rightarrow$ Lu s state excitations are observed at higher energy (≥ 3 eV). It is difficult to resolve all the excitations because they are

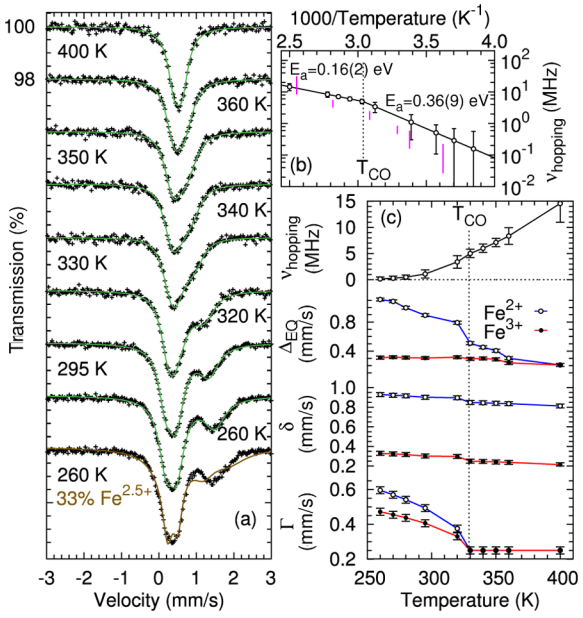

FIG. 1 (color online). (a) Mössbauer spectra of $LuFe_2O_4$ and fits, see text; bottom: alternative best fit with a constraint of 33% of hopping electrons (b) Arrhenius plot of the hopping frequency. Open symbols correspond to the spectra in (a), bars to hopping frequencies in [15]. (c) Mössbauer spectral parameters, from top to bottom: hopping frequency, quadrupole splitting, isomer shift, and full linewidth at half maximum.

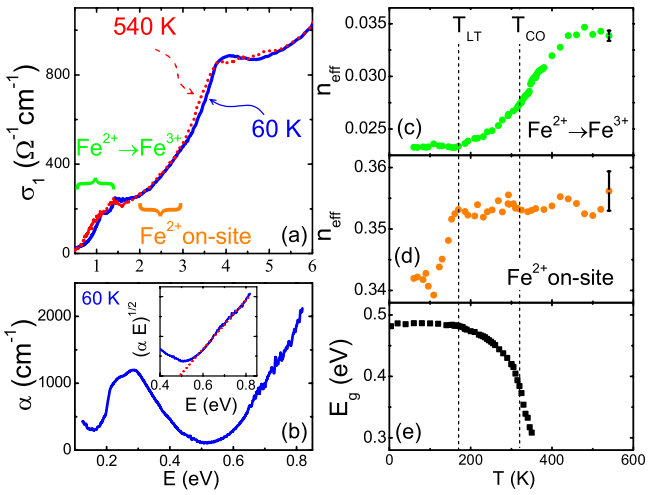

FIG. 2 (color online). Optical properties of $LuFe_2O_4$. (a) σ_1 vs energy E at 540 and 60 K calculated from a Kramers-Kronig analysis of reflectance. Brackets indicate assignments, the hierarchy determined from Ref. [7]. (b) α vs E calculated from transmittance, showing the charge transfer edge starting from ~0.5 eV. Inset: $\sqrt{\alpha E}$ with linear fit (dotted line). (c),(d) $n_{\text{eff}}(T)$ calculated by sum rules for $Fe^{2+} \rightarrow Fe^{3+}$ charge transfer (c) and Fe^{2+} on-site (d) excitations. (e) $E_g(T)$ calculated from an absorption edge fit assuming an indirect gap.

broad and overlap significantly. Nevertheless, the 1.1 eV peak in the near infrared range [Fig. 2(a)] can be associated with $Fe^{2+} \rightarrow Fe^{3+}$ charge transfer. The optical gap E_g is determined by the absorption edge of this band. A close-up view of the tail is shown in Fig. 2(b). The linear fit of $\sqrt{\alpha E}$ vs E above 0.5 eV indicates that the gap is indirect [13], in agreement with Ref. [17]. Because of the 0.3 eV feature (possibly a spin-forbidden Fe^{3+} on-site excitation [18]), the typical "double slope character" is not observed and the associated coupling phonon energy for the indirect gap excitation process can not be determined. The optical gap is sensitive to T_{CO} [Fig. 2(e)], although $LuFe_2O_4$ is a semiconductor (nonmetallic) over the full temperature range of our investigation.

To quantify the strength of the various excitations, we calculated the effective number of electrons n_{eff} from the optical conductivity $\sigma_1(\omega)$ using the partial sum rule: $n_{\text{eff}} \equiv \int_{\omega_1}^{\omega_2} \sigma_1(\omega)/\epsilon_0 d\omega / \frac{1}{2}\pi\omega_p^2$, where $\omega_p \equiv \sqrt{\frac{e^2}{V_0 m \epsilon_0}}$ is the plasma frequency, e and m are the charge and mass of an electron, ϵ_0 is the vacuum dielectric constant, V_0 is the unit cell volume, and ω_1 and ω_2 are the frequency limits of integration. The absolute level of n_{eff} depends on the integration range, but the temperature trends are not sensitive to this choice. For instance, to investigate changes in the Fe charge transfer band, we evaluated the partial sum rule from 0.6–1 eV, as indicated in Fig. 2(a). In this case, n_{eff} represents effective number of electrons that are able to overcome the energy barrier to hop from Fe^{2+} to Fe^{3+} sites. This number increases over a broad temperature range through T_{CO}, as shown in Fig. 2(c).

In optical processes, electrons hopping from Fe^{2+} to Fe^{3+} are better described as small polarons, which correspond to combined electronic and vibrational excitations that arise when the lattice is too slow to relax [19]. Important signatures include (i) a large effective mass and (ii) optical excitation energies that are much larger than the low frequency activation energy. The effective mass of the charge carriers can be estimated using $n_{\text{eff}} = \frac{m}{m^*} N$, where m^* is the effective mass and $N = 3$ (the number of Fe^{2+} site per unit cell). Considering that the 0.6–1 eV integration is only over half of the excitation, we get $\frac{m^*}{m} \approx 40$, which is large, but typical for polarons (e.g., $\frac{m^*}{m} \approx 100$ in Fe_3O_4 [10]). With the polaron picture and the simple model of an electron jumping between two sites [20], we can estimate the 60 K activation energy from the optical activation $\hbar\omega_0$ as $E_a = \hbar\omega_0/4 = 1.1(1)$ eV$/4 =$ 0.28(3) eV, in excellent agreement with value reported in the study of low frequency dielectric dispersion and dc electric conductivity ranging from 0.25–0.29 eV [2,15] and compatible with that for spontaneous electron hopping obtained between 260 and 320 K from Mössbauer spectroscopy.

The T dependence of n_{eff} corresponding to Fe^{2+} to Fe^{3+} charge transfer confirms charge fluctuation below T_{CO} [Fig. 2(c)]. Here, n_{eff} begins to increase well below T_{CO} (evident also in electron hopping trends via Mössbauer spectroscopy) and continues to change above this temperature. This result is consistent with the presence of 3D antiphase domain boundary modes [21]. We attribute the experimental observation of significant charge fluctuations through T_{CO} (even where diffraction shows that it is ordered) to relevance of the "order by fluctuation" mechanism in which fluctuations are needed to stabilize the $\sqrt{3} \times \sqrt{3}$ CO in the frustrated system [11]. Interestingly, the charge fluctuation onset is at T_{LT} [Fig. 2(c) and 2(e)], suggesting that the low-temperature phase transition quenches the charge fluctuation. Similar to the Verwey transition in Fe_3O_4 [22], the T dependence of n_{eff} shows an anomaly near T_{CO} consistent with the lowering of the activation energy above T_{CO} [15]. However, the jump occurs above T_{CO}.

The strength of the Fe^{2+} on-site crystal field excitation is quantified by the partial sum rule in energy range 2–3 eV, in accord with first principle calculations [7]. Although the data are more scattered than that discussed above because of the background from nearby excitations, two finding are immediately clear. First, the Fe^{2+} on-site excitation is rather insensitive to charge and spin ordering transitions. Second, it displays a clear anomaly at T_{LT} [Fig. 2(c)], which recent magnetization and neutron diffraction studies [9] identified as an additional first-order transition. Further magnetization measurements in $H \parallel c$ up to 7 T indicate

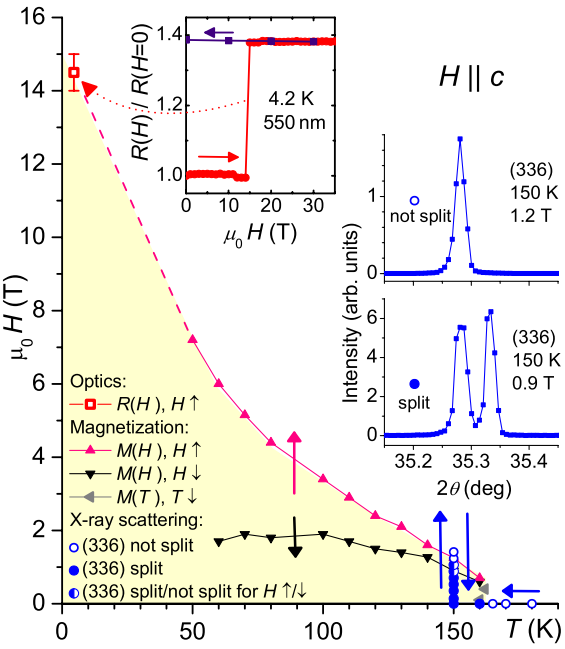

FIG. 3 (color online). Low-temperature phase transition from magnetization data (▲▼◀, see [9]), field-dependence of optical reflectance contrast $R(H)/R(H=0)$ at $\lambda = 550$ nm (squares, see left inset), and presence (indicated by ●) or absence (○) of a splitting in the total diffraction angle of the structural Bragg reflection (336) from synchrotron x-ray scattering (right insets). The maximum region of the structurally distorted phase is shaded (see text).

that the transition temperature is strongly suppressed by H (Fig. 3). Hysteresis of $H_{LT}(T)$ widens upon cooling, and below 50 K the high-H, high-T phase remains frozen in even after decreasing H to 0, reminiscent of kinetic arrest of first-order transitions as studied in doped $CeFe_2$ [23].

To check for possible [9] structural components of the transition, we closely examined structural Bragg reflections, such as (336). CO below 320 K lowers the crystal symmetry to monoclinic [8], which could lead to a monoclinic distortion ($\beta \neq 90°$), with a splitting in 2θ values of such reflections, with domain formation clearly observable also in single crystals [24]. Such a splitting could not be resolved in between 200 and 300 K (in any magnetic field), indicating that any monoclinic distortion is small. Splitting becomes evident upon cooling below T_{LT} (lower right inset in Fig. 3), consistent with a significant ($\beta \approx 90.5°$) monoclinic distortion [25]. Application of a magnetic field removes the splitting (upper right inset) as soon as the field component $\| c$ reaches H_{LT} as determined by magnetization, and subsequent reduction causes a reappearance of the splitting at a field value again consistent with magnetization. These diffraction data thus suggest that T_{LT} and $H_{LT}(T)$ corresponds to a strongly hysteretic magnetostructural transition. We propose that the monoclinic distortion removes geometric frustration rendering charge fluctuation unnecessary. This scenario is in line with the observed fluctuation onset at T_{LT} and the ''order by fluctuation'' mechanism.

The anomaly at T_{LT} in the Fe^{2+} on-site excitations can also be explained within a structural distortion scenario. Consider an Fe center coordinated by five O ligands in a trigonal bipyramidal geometry (D_{3d} symmetry). A crystal field splits the Fe $3d$ levels into three groups [11]. The monoclinic distortion in the low T phase splits these levels further, shifting the on-site excitation energies and causing the discontinuity in n_{eff} [Fig. 2(d)].

The upper-left inset in Fig. 3 displays the 4.2 K reflectance of $LuFe_2O_4$ at 550 nm as a function of magnetic field ($H \| c$). At this energy, the spectral response is probing field-induced changes in Fe^{2+} on-site excitations. Strikingly, the reflectance increases by $\sim$40% for $H \geq$ 14 T. This is consistent with a straightforward extrapolation of H_{LT} from the magnetization data (dashed line in Fig. 3). That the reflectance maintains this high value even after subsequent complete removal of H is again consistent with the magnetization data (see above). Thus, at low T a rather large field is required to switch the crystal structure. Since the structural distortion is most likely induced by the CO, which lowers the crystal symmetry [8], the strong H dependence of this transition is a further example of the strong coupling between spin, structural, and charge degrees of freedom in $LuFe_2O_4$.

In summary, optical and Mössbauer spectroscopies demonstrate that charge fluctuation in $LuFe_2O_4$ has an onset at T_{LT}, well below T_{CO}, supporting the ''order by fluctuation'' mechanism for the $\sqrt{3} \times \sqrt{3}$ CO superstructure. Fe^{2+} on-site crystal field excitations are sensitive to the magnetostructural transition at T_{LT}, which can be driven by both temperature and magnetic field (requiring 14 T at 4 K). Combining spectral, magnetic, and structural data, we generate a comprehensive H-T phase diagram. The large temperature range of the observed dynamical effects is a consequence of the strong coupling between charge, structure, and magnetism.

We thank the Division of Materials Sciences and Engineering and the Scientific User Facilities Division, Office of Basic Energy Sciences, U.S. Department of Energy for support of this work at UT, ORNL, and the APS. Work at the NHMFL is supported by NSF, DOE, and the State of Florida. Research at Liège is funded by the FNRS. We thank M. T. Sougrati for assistance with the Mössbauer and M.-H. Whangbo and H. Xiang for useful discussions.

[1] A. M. Kadomtseva *et al.*, JETP Lett. **79**, 571 (2004).
[2] N. Ikeda *et al.*, Nature (London) **436**, 1136 (2005).
[3] N. Shimamoto *et al.*, Inorg. Chem. **41**, 678 (2002); C. P. Berlinguette *et al.*, J. Am. Chem. Soc. **126**, 6222 (2004).
[4] N. Manyala *et al.*, Nature Mater. **3**, 255 (2004).
[5] Y. Kamihara *et al.*, J. Am. Chem. Soc. **130**, 3296 (2008).
[6] J. van den Brink and D. I. Khomskii, arXiv:0803.2964.
[7] H. J. Xiang and M.-H. Whangbo, Phys. Rev. Lett. **98**, 246403 (2007).
[8] M. Angst *et al.*, Phys. Rev. Lett. **101**, 227601 (2008).
[9] A. D. Christianson *et al.*, Phys. Rev. Lett. **100**, 107601 (2008).
[10] L. V. Gasparov *et al.*, Phys. Rev. B **62**, 7939 (2000).
[11] A. Nagano *et al.*, Phys. Rev. Lett. **99**, 217202 (2007).
[12] Z.-T. Zhu *et al.*, Phys. Rev. B **65**, 214519 (2002).
[13] F. Wooten, *Optical Properties of Solids* (Academic, New York, 1972).
[14] J. A. Tjon and M. Blume, Phys. Rev. **165**, 456 (1968).
[15] M. Tanaka, K. Siratori, and N. Kimizuka, J. Phys. Soc. Jpn. **53**, 760 (1984).
[16] Y. Zhang *et al.*, Phys. Rev. Lett. **98**, 247602 (2007).
[17] H. J. Xiang and M.-H. Whangbo (private communication).
[18] B. I. G. F. Henderson, *Optical Spectroscopy of Inorganic Solids* (Oxford University Press, New York, 1989).
[19] Y. Yamada, K. Kitsuda, S. Nohdo, and N. Ikeda, Phys. Rev. B **62**, 12167 (2000).
[20] I. G. Austin and N. F. Mott, Adv. Phys. **18**, 41 (1969).
[21] Y. Yamada, S. Nohdo, and N. Ikeda, J. Phys. Soc. Jpn. **66**, 3733 (1997).
[22] S. K. Park, T. Ishikawa, and Y. Tokura, Phys. Rev. B **58**, 3717 (1998).
[23] M. K. Chattopadhyay, S. B. Roy, and P. Chaddah, Phys. Rev. B **72**, 180401(R) (2005), and references therein.
[24] M. Angst *et al.*, Phys. Rev. Lett. **99**, 256402 (2007).
[25] The basic CO configuration appears the same with and without monoclinic distortion [8], but the magnetic structure is radically changed [9].